ISBN: 978-3-95450-241-7 ISSN: 2673-5350 doi:10.18429/JACoW-IBIC2022-TUP09

DESIGN OF THE BEAM POSITION MONITOR FOR SOLEIL II

M. El Ajjouri, N. Hubert, A. Gamelin, F. Alves, Synchrotron SOLEIL, Saint-Aubin, France

Abstract

The Beam Position Monitors (BPM) for the SOLEIL low emittance upgrade project (SOLEIL II) are currently in the design phase. Efforts are put on the minimization of the heat load on the button by optimizing the longitudinal impedance and the BPM materials.

To validate the mechanical design and tolerances, a first prototype has been manufactured and controlled. This paper presents the mechanical design of the BPM, the metrology of the prototype and the lessons learned from this prototyping phase.

INTRODUCTION

SOLEIL is the French third generation light source routinely operated for external users since 2008 with electron beam emittance of 4 nm·rad at an energy of 2.75 GeV and a nominal current of 500 mA (uniform filling pattern). A low emittance upgrade project is currently in the Technical Design Report (TDR) phase. The reference lattice features a natural emittance of 84 pm.rad [1, 2]. It is based of alternating 7 bend and 4 bend achromats to minimize the displacement of the current source point and realignment of the beamlines, keeping the tunnel shielding wall unchanged. Main comparison lattice parameters are listed in Table 1.

Table 1: Main baseline TDR lattice parameters

	SOLEIL	***SOLEIL II***
Circumference (m)	354.1	353.9
Beam energy (GeV)	2.75	2.75
Beam current (mA)	500	500
Lattice Type	DBA	7BA/ 4BA
Straight section number	24	20
Natural emittance (pm·rad)	4000	84
RMS Nat. Bunch length (ps)	15	9
RF Voltage (MV)	2.8	1.8
RF Frequency (MHz)	352.2	352.4
Vacuum chamber size (mm)	70/25	12 round

BPM SPECIFICATIONS

SOLEIL II storage ring will be equipped with 180 BPMs: 7 per 4BA section, 10 per 7BA section and 4 additional BPMs in the two long straight sections (Fig. 1).

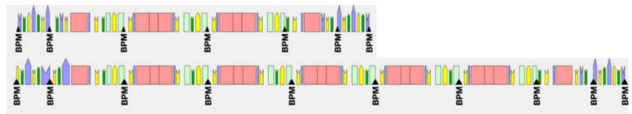

Figure 1: 4 BA cell (up) and 7 BA cell (down), and the beam position monitor location on the SOLEIL II lattice.

The main BPM specifications are listed in Table 2.

Table 2: Main Specification of the Beam Position Monitors

	Time scale/freq.	***Specifications***
Number of BPM		~180
BPM radius		16 mm
BPM resolution	@10 Hz @100 kHz TbT	1 µm@0.1 mA 50 nm@500 mA 100 µm@0.1 mA 1 µm@500 mA
Beam current dependence	0.1-20 mA in a single bunch	10 µm
Stability	One day One week	500 nm 1 µm
Absolute accuracy before BBA		<500 µs

BPM BLOCK MECHANICAL DESIGN

BPM Mechanical Integration

SOLEIL II vacuum chambers will have a drastically small inner diameter of 12 mm to allow high gradients in the quadrupoles and sextupoles. To keep the BPM body in the shadow of the bending magnets synchrotron radiation, their inner diameter will be enlarged to 16 mm. Systematic tapers upstream/downstream each BPM will ensure a smooth transition between the two pipe diameters.

A large part of the bending magnet synchrotron radiation power will be intercepted (and absorbed) by the vacuum chambers. To minimize the mechanical stress induced by the vacuum chambers during the thermalization of the machine, the straight section BPM will be isolated with bellows. In the arcs, due to high component density, only one bellow between two BPMs is foreseen. All the BPMs will be the fixed points of the vacuum chamber with rigid supports connected either to the ground (straight sections) or the girders (in the arcs).

To achieve the long-term stability requirements of 500 nm a day, 1 µm a week, and considering a temperature in the tunnel stabilized at ±0.1 °C, low thermal expansion stands will be considered in the straight sections. Invar is

ISBN: 978-3-95450-241-7 ISSN: 2673-5350 doi:10.18429/JACoW-IBIC2022-TUP09

the best candidate. As shown in Fig. 2, its thermal expansion would remain below 300 nm for a 1.2 m heigh stand.

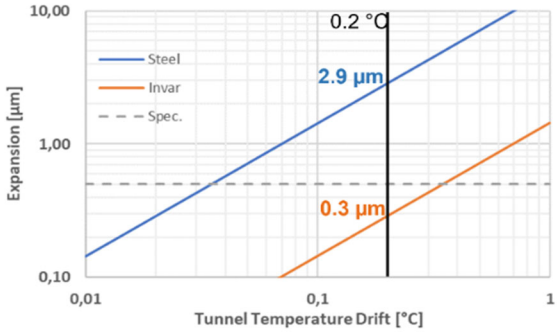

Figure 2: Expansion of 1.2 m heigh stand made of Invar (orange) and steel (blue). Steel stand would not fit our 24h stability requirement below 500 nm.

Button Design Optimization

The heating of the button due to the trapped fields is an important aspect to take care in the design. Optimization of the longitudinal impedance by adapted feedthrough geometry and materials allows to reduce significantly the power deposited on the button. Usual optimisation of the different parts of the feedthrough (button, ceramic and gap dimension) have been studied and published in [3].

Additional possible ways of improving the longitudinal impedance have been investigated for SOLEIL II button BPM. Based on the work carried out on the optimisation of the BPM impedance of Sirius [4], we compared the usual straight button shape (90° angle) with a conical one (65° angle) (Fig. 3).

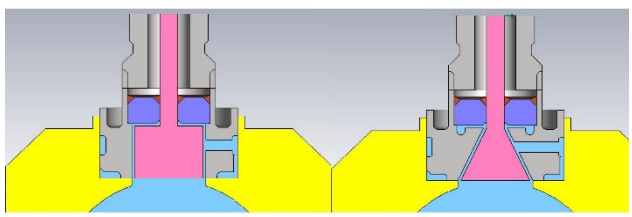

Figure 3: Schematics of two different button geometries: 90° button shape (left) and 65° (conical) button shape (right).

With the conical shape trapped modes are shifted to higher frequencies (Fig. 4).

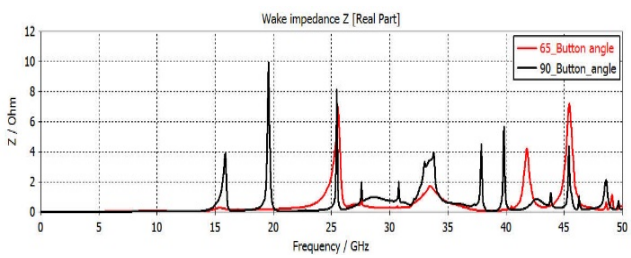

Figure 4: The real part of longitudinal impedance for different button geometry: black 90° button angle, red 65° button angle computed by CST Studio Suite [5].

SOLEIL II main operational mode will be 500 mA distributed uniformly in the 416 bunches. Bunches will be lengthened up to about 30 ps rms using a harmonic RF cavity. In case of a failure of this cavity, the power deposited on the BPM for a bunch length of 10 ps rms has also been studied.

For bunch length of 10 ps rms, the conical shape button will have 37% less power deposited compared to the straight one. For bunch length of 30 ps rms, the conical button is slightly worse than the 90° one but deposited power remains very low (0.15 W on the 4 buttons). (See Table 3).

Table 3: Power Loss Versus Button Shape

Button shape	conical	straight
Pl(mW) @(σ=30 ps rms)	150	100
Pl(mW) @(σ=10 ps rms)	2200	3020

The calculation of the spectral distribution of the power dissipated in the BPM shows that significant peaks are around 15 and 20 GHz for the straight button (Fig. 5), while for the conical button the peak is around 25 GHz. The maximum amplitude of the spectrum is three times greater for straight button than the conical button (0.36 W against 0.12 W).

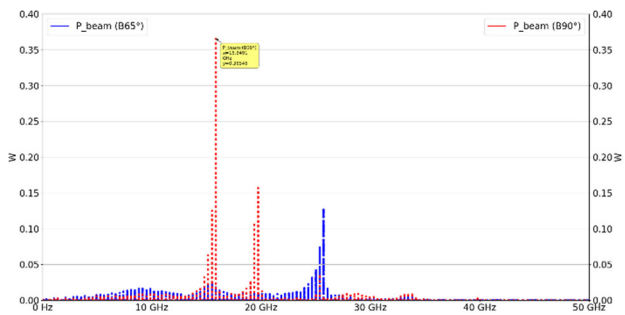

Figure 5: The spectral distribution of the power dissipated in the BPM (blue) for the 65° button and (red) 90° button.

3D simulations of the trapped mode surface current at 25 GHz for 10 ps rms bunch length confirm that the charge circulation at this frequency is well located on the button surface (Fig. 6).

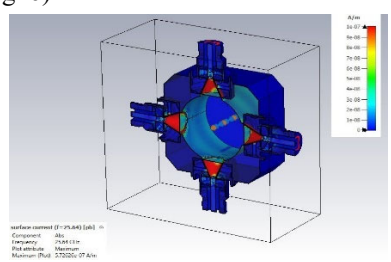

Figure 6: Trapped mode at 25 GHz for 10 ps rms bunch length.

Materials Considerations

When the trapped modes are excited, circulating charges around the button and its housing will heat the materials.

ISBN: 978-3-95450-241-7 ISSN: 2673-5350 doi:10.18429/JACoW-IBIC2022-TUP09

The distribution of deposited power is made accordingly to the conductivity of the materials used for the button and its body. This is proportional to the ratio of the square roots of electrical conductivity [6]: if the materials are identicals, the power is equally distributed, but if the electrical conductivity of the button is higher than the one of the body, the power deposition will be enhanced on the body instead of the button. For example, in the case of molybdenum button and stainless-steel body only 26% of the heating power will go on the button (Table 4). On the contrary a low conductivity material should be avoided for the button.

Table 4: Distribution of Power Deposited in the Button According to the Materials

Body \ Button	Molybdenum	Copper	316LN
Molybdenum	50%	46%	75%
Copper	64%	50%	85%
316LN	26%	15%	50%

Chromium Zirconium Copper (CuCrZr) is foreseen for SOLEIL II vacuum chamber material and eventually also for the BPM blocks. Copper is not adapted for a button housing due to its high electrical conductivity. Nevertheless since the feedthrough design has its own button housing, a different material as stainless steel can be chosen for this part.

The impedance simulation and the power loss in the BPM is much better for the CuCrZr body than the stainless steel. Impedance at low frequency (resistive wall) is much lower in the case of a BPM with the copper body compared to stainless steel (Fig. 7).

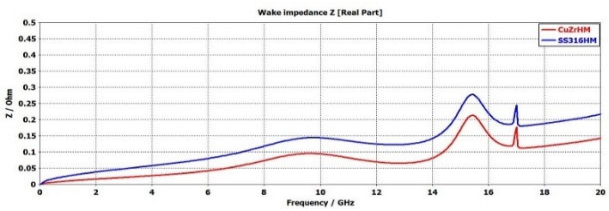

Figure 7: Real part of longitudinal impedance (in blue 316LN and in red CuCrZr).

The calculation of the dissipated power in Table 5 shows a very significant difference between the two materials.

Table 5: Total power loss versus BPM body's materials (button is in molybdenum, and button housing in stainless steel)

Power loss	SS316LN	CuCrZr
σ=30 ps rms (mW)	320	150
σ=10 ps rms (mW)	3000	2200

PROTOTYPING

To validate the mechanical design of the feedthrough and its integration in the BPM body, we have manufactured a batch of twelve buttons based on our design. (Fig. 8).

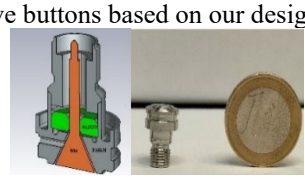

Figure 8: New BPM Feedthrough. The button diameter is 5 mm and the gap between buttons and its housing is 200 µm.

Metrology

Careful metrology has been carried on to check the mechanical tolerances and qualify the mechanical manufacturing. With such small pieces, traditional mechanical metrology tools are not well adapted, and we employed optical methods to measure the different dimensions like the button diameter and flatness, its concentricity and retreat with respect to its housing. Microscope pictures and images analyse software [7] has been used in addition to interferometer measurements (Fig. 9).

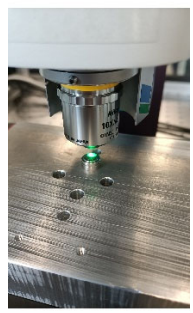

Figure 9: White light Interferometry (WLI) measurement of the button flatness and position.

The measurements show that some buttons present a tilt with respect to the external body (Fig.10).

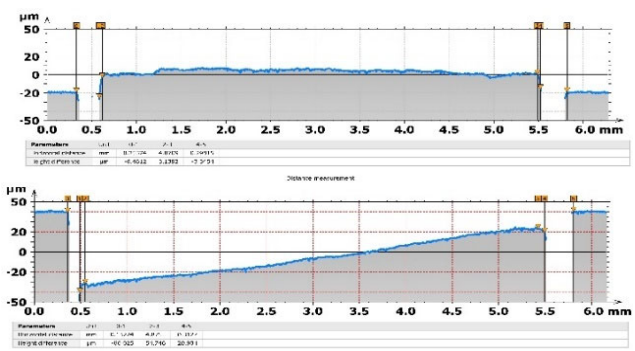

Figure 10: Flatness observed to button up good flatness and down bad flatness.

This tilt directly affects the gap between the button and its body. This variation of the gap is confirmed by microscope observations (Fig. 11). This tilt is due to a mechanical shift of the button during the brazing process. Future

ISBN: 978-3-95450-241-7 ISSN: 2673-5350 doi:10.18429/JACoW-IBIC2022-TUP09

design will be adapted in order to improve the way of maintaining the button at the right position at brazing.

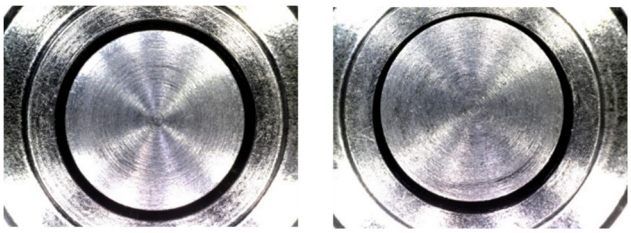

Figure 11: Microscope picture of two buttons, one with a good concentricity (left) and another one with an important concentricity error due to a tilt of the button (right).

Capacitance Measurement

Button capacitance has been measured with a Time Domain Reflectometer (TDR). All buttons shown a similar capacitance (~4 pF) except the one that had the biggest concentricity error for which the capacitance is sensitively different (5.3 pF) (Fig. 12).

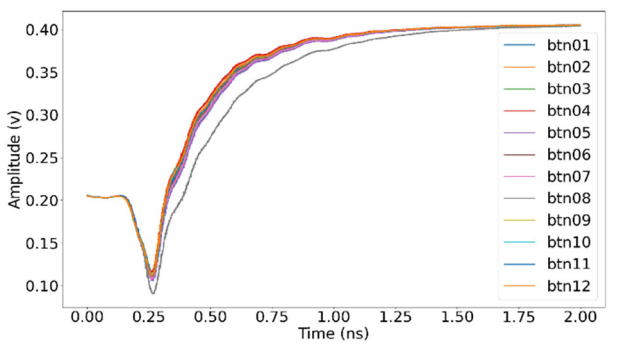

Figure 12: Button capacitance measurement with TDR.

This measure will allow us to relax certain tolerances such as button concentricity, tilt and gap imposed for the future buttons manufacturing.

Button Welding

Two batches of 4 buttons have been selected depending on their metrology measurements. Each batch has been welded on a BPM block manufactured in-house. A dedicated mechanical positioning system prevents any displacement of the button during the welding procedure (Fig. 13).

Figure 13: The welding process(left), the current BPM size and the new BPM (right).

BPM Calibration

The electrical offset of the BPM has been measured with the Lambertson method [8]. This method uses the coupling between buttons/electrodes to determine the gain factors of each electrode. The ratios between gain factors provide the difference between the mechanical and electrical centers. The measurement has been made at 352 MHz with a 4-port Vector Network analyser (Fig. 14). Table 6 summarizes the S-parameter matrix for the BPM prototype 1.

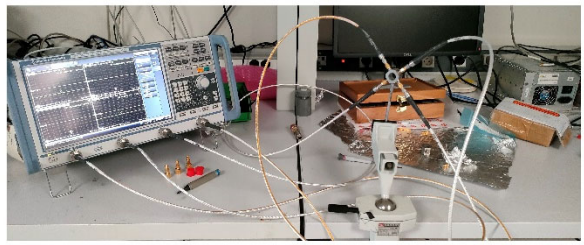

Figure 14: The electrical offset measurement setup.

Table 6: S Parameter Matrix (dB) for BPM Prototype N°1

Port	1	2	3	4
1		-81.6979	-89.1576	-81.5442
2	-81.7720		-81.5876	-89.7595
3	-89.1834	-81.6291		-81.4207
4	-81.5856	-89.7807	-81.4792	

Table 7 resumes the electrical offset obtained for both prototypes.

Table 7: Electrical Offset Calculated from S Parameter Matrix

	Prototype1	Prototype 2
X Offset	20 µm	2 µm
Y Offset	-45 µm	10 µm

Resulting offsets are very small and well within specifications (absolute accuracy of the BPM system <500 µm). There is nevertheless a discrepancy with those expected from the button metrology measurements and their arrangement on the BPM blocks. Investigations are ongoing to understand the reason.

CONCLUSION

The manufacturing of these buttons is a first step in the validation of the conical shape design. Several ways of improvements have already been identified with the manufacturer for a second design version, working on the mechanical but also on the production cost aspects.

In the near future, vacuum flanges will be welded on the BPM block prototypes for vacuum testing, as well as for NEG coating validation.

ACKNOWLEDGMENT

The authors would like to express our very great appreciation to Dr Kubsky and his team for their valuable and constructive suggestions during the button's metrology. We would like also to thank the mechanical and vacuum groups for their participation in the project.

ISBN: 978-3-95450-241-7 ISSN: 2673-5350 doi:10.18429/JACoW-IBIC2022-TUP09

REFERENCES

[1] Synchrotron SOLEIL "Conceptual Design Report", https://www.synchrotron-soleil.fr/en/file/13803/download?token=OUzsp46P

[2] A. Loulergue *et al.*, "TDR Baseline Lattice for the Upgrade of SOLEIL", in *Proc. IPAC'22*, Bangkok, Thailand, Jun. 2022, pp. 1393-1396. doi:10.18429/JACoW-IPAC2022-TUPOMS004

[3] M. El Ajjouri, F. Alves, A. Gamelin, and N. Hubert, "Preliminary Studies for the SOLEIL Upgrade BPM", in *Proc. IBIC'21*, Pohang, Korea, Sep. 2021, paper MOPP31, pp. 128

[4] H. O. C. Duarte, S. R. Marques, and L. Sanfelici, "Design and Impedance Optimization of the SIRIUS BPM Button", in *Proc. IBIC'13*, Oxford, UK, Sep. 2013, paper TUPC07, pp. 365-368.

[5] https://www.3ds.com/products-services/simulia/products/cst-studio-suite/electromagnetic-systems/

[6] I. Pinayev and A. Blednykh, "Evaluation of Heat Dissipation in the BPM Buttons", in *Proc. PAC'09*, Vancouver, Canada, May 2009, paper TH5RFP014, pp. 3471-3472.

[7] https://www.digitalsurf.com/software-solutions/profilometry/

[8] W. X. Cheng, B. Bacha, and O. Singh, "NSLS2 Beam Position Monitor Calibration", in *Proc. BIW'12*, Newport News, VA, USA, Apr. 2012, paper MOPG022, pp. 77-79.